Supporting Information

Poly(Ionic liquid)-zinc polyoxometalate composite as binder free cathode catalyst for high performance lithium-sulfur battery

Vikram Singh, Anil Kumar Padhan, Subhasis Das Adhikary, Aarti Tiwari, Debaprasad Mandal* and Tharamani C. Nagaiah*

Department of Chemistry, Indian Institute of Technology Ropar, Rupnagar, Punjab-140001, India

Experimental:

***General*:** Glassware used in the experiments were thoroughly washed and dried in oven before use. Composite and its precursors were vacuum dried at ~60 °C under 10^{-3} m bar pressure for 2 h to ensure the maximum evaporation of free water molecules and volatile substances (if present in sample) before performing each test.

***Materials**:* All the reagents were used as received. $Na_2WO_4.2H_2O$ (98%), $Zn(NO_3)_2.6H_2O$ (98%) α,α'-Azoisobutyronitrile (98%), 1-vinylimidazole (99%), HCl, H_2SO_4 (Alfa Aesar). Aqueous solutions were prepared using deionized water from Millipore system (>12 MΩ cm^{-1}).

***Synthesis of 4*:** A RB flask was charged with 2-(2-methoxyethoxy)ethanol (23.8 mL, 175.00 mmol), 200 mL of THF and followed by powdered NaOH (7.200 g, 180.00 mmol). The reaction was stirred at ambient temperature for 1 h. *p*-toluene sulphonyl chloride (42.504 g, 223.00 mmol) was added by pinch at 0 °C. Immediately, a copious precipitate was formed and mixture was refluxed under N_2 for 24 h. The reaction progress was checked by TLC in 30% ethyl acetate in hexane. After completion the reaction mixture was filtered and maximum THF was evaporated in *rotavac.* The filtrate was extracted with dichloromethane (100 mL × 3) and organic phase was dried on Na_2SO_4. Solvent evaporated to give yellow oil and purified by flash column chromatography. Afforded pure colorless liquid (**3**, 41.278 g, 150.48 mmol, 86%) as shown in Scheme S1. Compound **3** was used in subsequent reaction without any further purification. Compound **3** was mixed with NaBr in dry acetone and refluxed for 48 h. The reaction progress was checked by thin layer chromatography technique. After completion, the reaction mixture was

filtered and evaporated the acetone to minimum under *rotavac*. The slurry was extracted from dichloromethane and distilled water (100 mL × 3) and the organic phase was dried over Na_2SO_4 gives **4** (2-(2-methoxyethoxy)ethyl bromide) as colourless liquid which was further purified by distillation.

NMR (^{1}H, $CDCl_3$) δ ppm: 7.79 (d, *J*=8.3 Hz, 2H, *Ar*-C*H*C*H*), 7.33 (d, *J*=8.0 Hz, 2H, *Ar*-C*H*C*H*), 4.15 (t, *J*=4.8 Hz, 2H, SOCH_2CH_2O), 3.68 (t, *J*=5.0 Hz, 2H, SOCH$_2$CH_2O), 3.51 (m, 2H, OCH_2CH_2O), 3.49 (m, 2H, OCH$_2$CH_2O), 3.34 (s, 3H, OCH_3), 2.44 (s, 3H, *Ar*-CH_3).

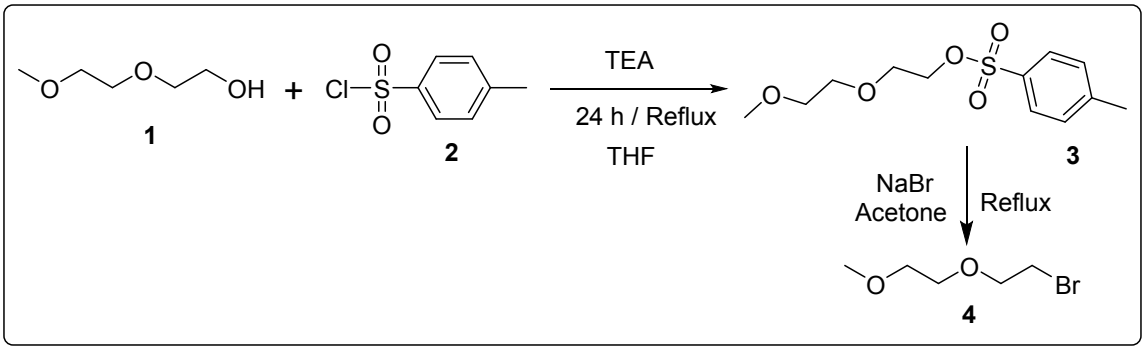

Scheme 1. Synthesis of **4**

Synthesis of polymer 6: Monomer vinyl imidazole (0.941 g, 10.0 mmol), AIBN (Azobis isobutyronitrile; 1.0 wt%, 13.14 mg) and 4 mL of dry toluene were charged in 50 mL Schlenk tube. The reaction mixture was degassed in three thaw freeze cycles under high vacuum (0.1 mbar pressure) to remove oxygen followed by purging argon for 30 min. The obtained reaction mixture was heated at 70 °C. After 24 h of the reaction, a solid precipitate was formed. The precipitate was purified by precipitation with acetone and dried under vacuum (1×10^{-3} mbar) at 60 °C for 24 h to afford **6** (0.751 g, 80%).

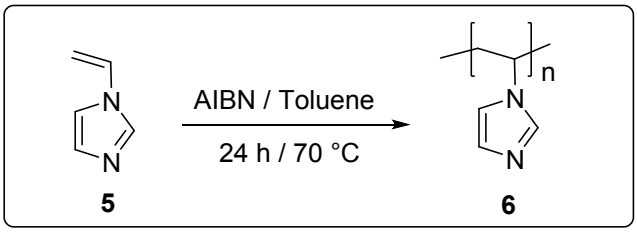

Scheme 2: Synthesis of poly(vinyl imidazole) (**6**)

Synthesis of polymer 7: Poly(vinyl imidazole) **6** (0.339 g, 3.62 mmol), **4** (0.543 g, 3.98 mmol) and dry methanol (1.0 mL) was taken in a 50 mL Schlenk tube fitted with condenser and heated the mixture at 70 °C for 48 h. After completions of reaction, the product was purified by precipitation with acetone and dried under vacuum (1×10^{-3} mbar) at 60 °C for 24 h to **yield** 92.3 wt% **7** [Poly(1-vinyl butyl imidazolium bromide) (PVIMoBr).

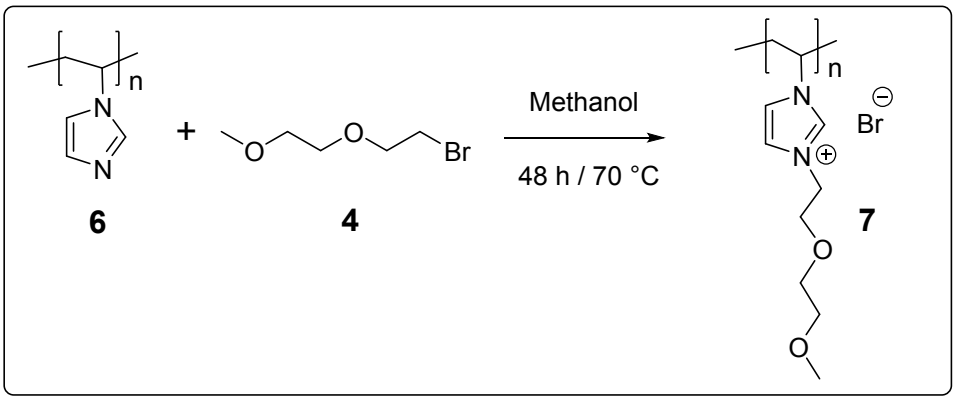

Scheme 3: Synthesis of ionic polymer **7**

Synthesis of $Na_{12}[WZn_3(H_2O)_2(ZnW_9O_{34})_2]$. $[Na_{12}(ZnPOM)]$: This has been synthesized according to our previous report.[1] Briefly, a two-neck round bottom flask fitted with a condenser was charged with $Na_2WO_4.2H_2O$ (7.599 g, 23.04 mmol) and dissolved in 24 mL of water. The solution was treated with 1.75 mL HNO_3 (10 N) at 80-85 °C under vigorous stirring until the initial precipitate dissolved completely. A solution of $Zn(NO_3)_2.6H_2O$ (1.784 g, 6.00 mmol) in 6 mL of distilled water was added dropwise, under vigorous stirring and heating at 90-95 °C (without boiling). A white precipitate was formed which re-dissolved immediately. The addition was controlled in such a way so that reaction mixture remained clear till the end of addition. The pH of reaction mixture was ~7.5. The reaction mixture was allowed to cool to room temperature and the clear solution was evaporated to half the volume. White needle-like crystals were formed on standing for 2 days. Crystalline compounds were collected by filtration. The compounds were recrystallized from water and dried under vacuum to give Na_{12}[ZnPOM] (1.562 g, 0.29 mmol, (50.9%).

Synthesis of (PVIMo)$[WZn_3(H_2O)_2(ZnW9O_{34})_2]$ (PVIMo-ZnPOM Composite): A Schlenk tube was charged with Na_{12}[ZnPOM] (0.114 g, 0.02 mmol) and dissolved in 4 mL of water. A solution

of **PVIMoBr** (0.204 g, 0.88 mmol) in 5 mL of water was added slowly and immediately a white emulsion was formed, which was heated at ~80 °C for 2 h. The emulsion suspension was cooled to room temperature and filtered through frit and dried under vacuum to give PVIMo-ZnPOM (85%).

***Preparation of Li_2S_4 and Li_2S_6 (LiPS)**:* The LiPS solution was prepared by following the reported procedure.[2] Briefly, desired stoichiometric amount of S, Li_2S and $LiNO_3$ (5 wt%, as Li source to balance the counter ion) were dissolved in the mixture of 1,3-dioxolane (DOL) and dimethoxyethane (DME) (1:1 v/v). For a typical preparation of 5 M LiPS solution, 0.55 g of sulfur and 0.12 g of Li_2S were added to 4 mL of the mixture of DME and DOL (1:1) electrolyte. The obtained suspension was stirred and heated at 80 °C overnight to yield red-brown LiPS solution.

***Preparation of PVIMo-ZnPOM/Sulfur, PVIM-ZnPOM/Sulfur and Vulcan carbon/sulfur composite*:** The incorporation of sulfur in the PVIMo-ZnPOM composite was done by following melt-diffusion method.[3] Briefly, the desired ratio of PVIMo-ZnPOM composite with sulfur were physically grinded and heated at 150 °C for the incorporation of sulfur. PVIM-ZnPOM and Vulcan carbon/sulfur was prepared *via* same melt-diffusion process with same quantity of sulfur content.

Electrochemical Characterization

***Cell assembly & electrochemical measurements*:** Cathode was prepared by mixing 30:10:60 wt% PVIMo-ZnPOM, Vulcan carbon and elemental sulfur respectively. The obtained mixture was homogenized by grinding in a mortar-pestle and was further used to prepare the cathode slurry using appropriate amount of N-Methyl-2-pyrrolidone (NMP) to form a stable slurry designated as PVIMo-ZnPOM/C/S which served as binder free cathode wherein PVIMo, the polymer matrix act as binder. The prepared slurry was applied onto the aluminum foil (Ø 0.55 cm) current collector with an average loading of 2.6 mg which served as cathode in the assembled Li-S battery. PVIM-ZnPOM and Vulcan carbon-based cathode with similar sulfur weight percentage were also prepared by following the aforesaid procedures.

The battery analysis was performed by compiling a Lithium-sulfur cell using Swagelok T-cell in an argon filled glove box with lithium as anode and synthesized PVIMo-ZnPOM/C/S as cathode. Whatman filter paper served as a separator and 10 μL of electrolyte composed of 1 M LiTFSI (Lithium bis(trifluoromethanesulfonyl)imide), in a 1:1 v/v mixture of 1,3-dioxolane (DOL) and

dimethoxyethane (DME). In addition, to understand the effect of electrolyte on the performance of battery, few measurements were also performed at higher volume of electrolyte. After the compilation of battery, charge-discharge analysis was performed at different current rates in the potential range between 2.9 to 1.4 V *vs.* Li/Li^+ using battery cycler (BCS-810, Biologic).

Electrocatalytic activity of PVIMo-ZnPOM/C and Pt/C using Li_2S_6 in electrolyte: The electrochemical measurements were performed using Biologic VSP300 modular potentiostat/ galvanostat with an FRA7M module, controlled by EC-Lab V11.12 software in a three-electrode assembly wrapped in an inert glove box bag. The glassy carbon electrode (GCE, Ø5 mm) was used as a working electrode, lithium metal as reference and graphite as counter electrode respectively. Before each analysis, GC was polished to achieve mirror finish using Nylon polishing cloth (SM 407052, AKPOLISH) with different grades of alumina paste (3, 1, 0.3 and 0.05 mm; Pine Instrument, USA) followed by thorough washing and ultrasonication to remove an adsorbed impurities and alumina particles.

The working electrode mainly consist of PVIMo-ZnPOM/C or Pt/C over glassy carbon electrode and was prepared by drop casting 50 µL slurry of PVIMo-ZnPOM/C (30:70 ratio w/w) and Pt/C (20%). The 10 mL solution of Li_2S_6 (10 µL) was prepared in DME: DOL (1:1 v/v) using 1 M LiTFSI. Further cyclic voltammogram was performed for each catalyst at a scan rate of 5 mV/s.

Electrochemical quartz crystal microbalance (EQCM): The EQCM analysis was performed in a single compartment, three-electrode cell having Au-mesh as counter and Ag/Ag^+ as reference and thin Au film (Au film deposited on 6 MHz AT-cut quartz crystal (Metrohm) as working electrode respectively. The working electrode was prepared by drop casting PVIMo-ZnPOM/C/S (50 µL) over thin Au film. The EQCM measurements were performed in an electrolyte containing a mixture of DME: DOL (1:1 v/v) using 1 M LiTFSI as an electrolyte. Cyclic voltammetry experiments were performed at a scan rate of 1 mV/s. The change in resonance frequency of the quartz crystal electrode was simultaneously measured along with the current in an applied potential range of 2.7 to 1.8 V (*vs.* Li/Li^+) at a scan rate of 1 mV/s. According to the Sauerbrey's equation,[4] the corresponding mass change (Δm) was derived from the observed frequency change (Δf);

$$\Delta m = -C_f \Delta f$$

Where, C_f is the sensitivity factor of 6 MHz AT-cut quartz crystal whose theoretical value is 12.3 ng/Hz cm^2.

***Morphology and elemental analysis**:* Morphology of the PVIMo-ZnPOM/C/S cathode before and after charge-discharge analysis were performed using Field emission scanning electron microscope (FE-SEM, ZEISS, ULTRA PLUS) and transmission electron microscope (TEM, FEI Tecnai (G2 F20) operating at 200 keV). The elemental analysis was performed using energy dispersive X-ray analysis (EDX; Oxford, INCAx-act, 51-ADD0013).

X-ray photoelectron spectroscopy (XPS) measurements were performed using monochromatic Al Kα radiation (1486.6 eV) using Scienta R4000 hemispherical electron analyzer. The measurements were performed at a pass energy of 200 eV. The spectra were calibrated with respect to C (1s) peak at 284.5 eV with a precision of ±0.2 eV.

Sample preparation: The cathode was retrieved after specified number of cycles either in charged or discharged status by dissembling the cell in the glovebox. Further, retrieved electrodes were washed with acetonitrile thrice to remove the impurities (soluble polysulfide's and lithium salt) onto the surface of the electrode, followed by drying for 1 h under vacuum and used for further analysis.

***Polysulfide adsorption study**:* In order to analyze the interaction between prepared composite with LiPS, adsorption study was performed for PVIMo-ZnPOM and Vulcan carbon by considering Li_2S_4 as symbolic polysulfide in the electrolyte. The Li_2S_4 solution was prepared by dissolving 4 mg of Li_2S_4 in 4 mL DME and DOL (1:1, v/v) mixture which resulted in yellow coloration of the electrolyte. In each solution, 10 mg of the sample of interest was added followed by stirring for 1 h. It was observed that in case of PVIMo-ZnPOM composite the yellow color of Li_2S_4 start disappearing immediately upon addition and completely disappears after few hours (Figure 3b, manuscript), indicating strong interaction. Whereas, case is *vice-versa* for Vulcan carbon (Figure 3c, manuscript) where no disappearance of yellow color was observed even after allowing the mixture to stand for overnight, confirming unavailability of interactive sites towards Li_2S_4 adsorption. Further, each sample was retrieved by centrifugation and subsequent washing which was further used for FT-IR.

FT-IR analysis: FT-IR spectra were recorded using BRUKER TENSOR-27 spectrometer in the range of 600−4000 cm^{-1} with spectral resolution of 4 cm^{-1} and number of scans 100. FT-IR data was collected and analyzed by OPUS data collection and analysis software.

UV-visible analysis: UV-vis. spectra were recorded using the Shimadzu UV-2600 spectrophotometer by using $BaSO_4$ as the standard reflectance sample.

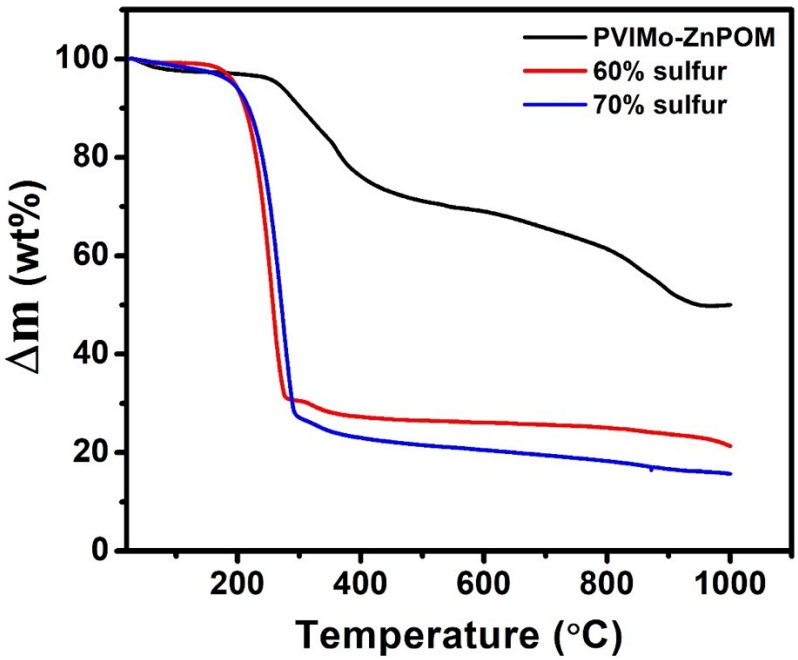

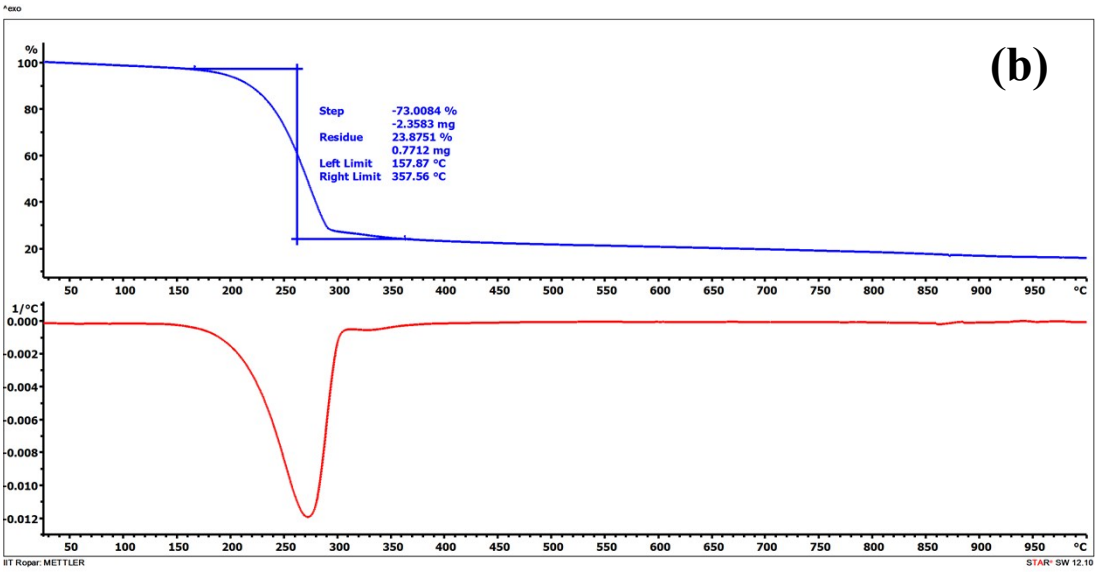

Figure S1. (a) Thermogravimetric analysis (TGA) for PVIMo-ZNPOM and PVIMo-ZNPOM/VC/S (60 and 70% loading of sulfur) and (b) derivative thermogravimetric (DTG) curve of PVIMo-ZNPOM/VC/S (70% loading of sulfur).

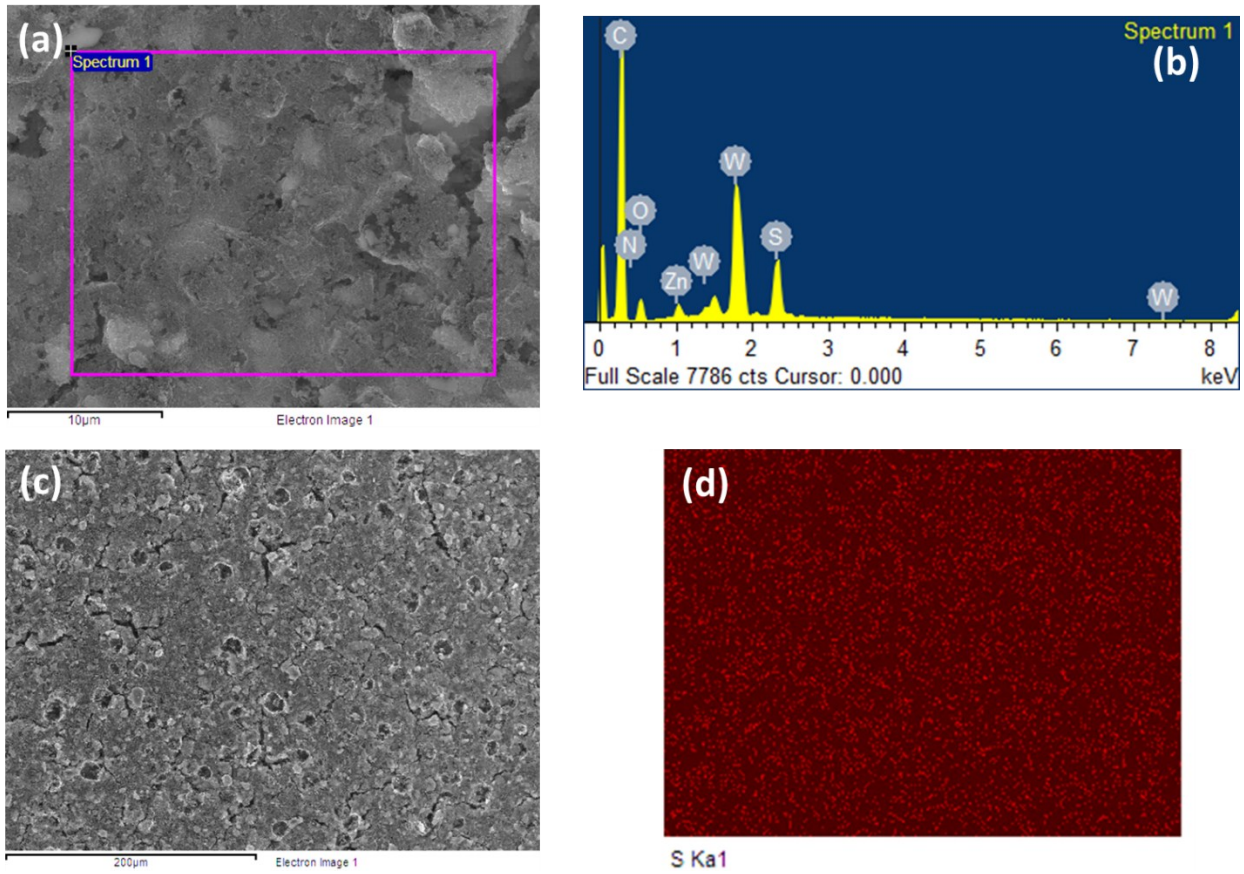

Figure S2. (a) SEM image and (b) corresponding EDX spectrum of PVIMo-ZnPOM/C/S cathode; (c) FE-SEM image with corresponding and (d) EDX dot-mapping of sulfur of PVIMo-ZnPOM/C/S cathode.

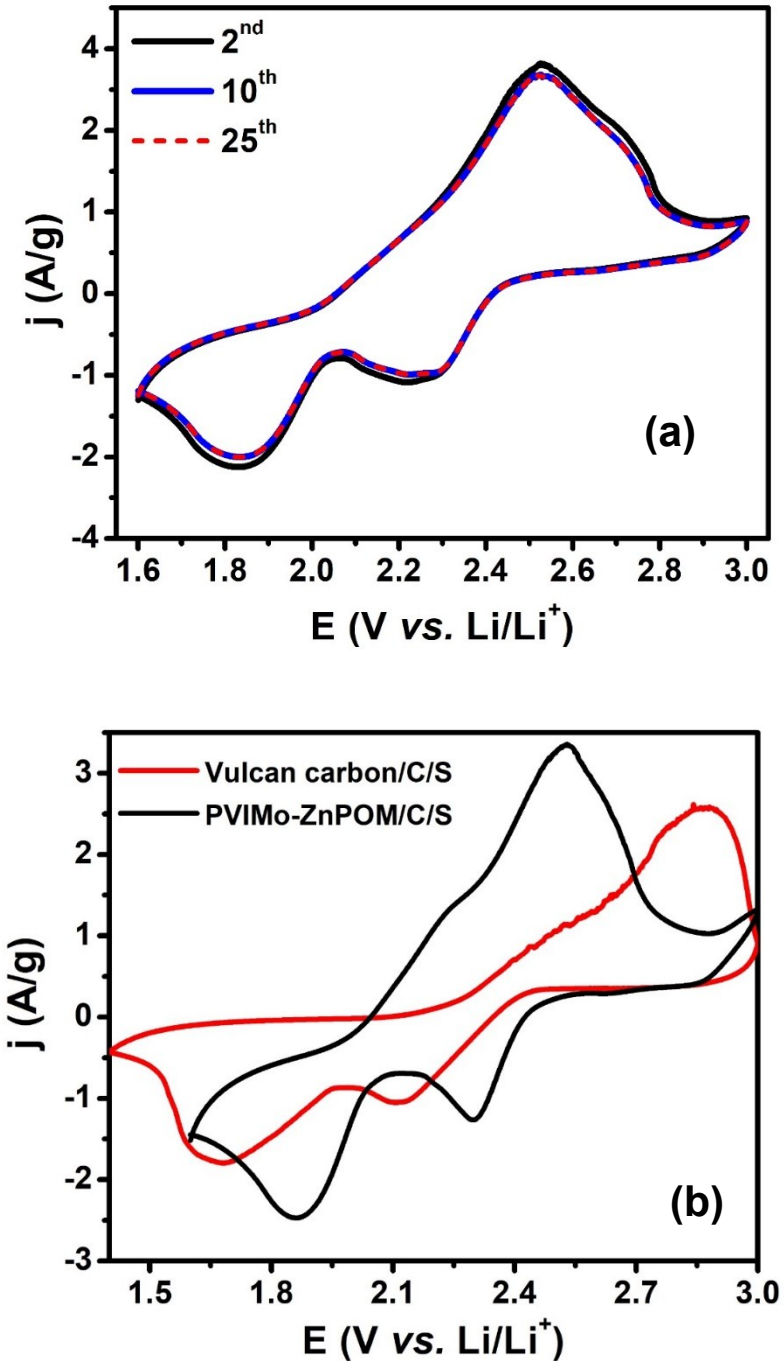

Figure S3. (a) Cyclic voltammogram of PVIMo-ZnPOM/C/S cathode at a scan rate of 0.5 mV/s. (b) A comparative cyclic voltammogram (10^{th} cycle) for PVIMo-ZnPOM/C/S composite *vs.* VC/S for kinetic analysis at a scan rate of 0.5 mV/s.

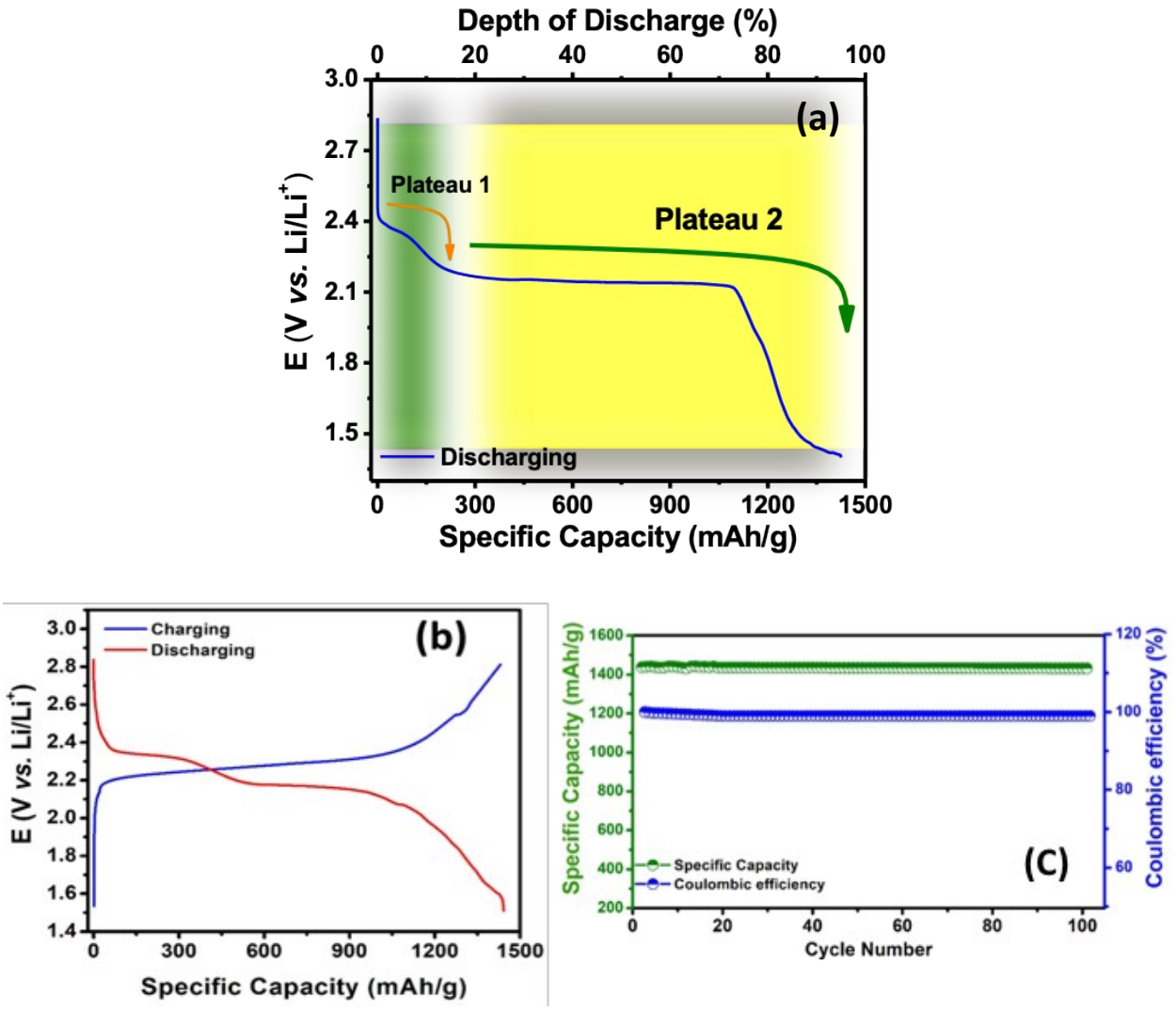

Figure S4. Galvanostatic charge-discharge along with depth-of-discharge for PVIMo-ZnPOM/C/S cathode at 0.5C rate (60% sulfur). (b) Galvanostatic charge-discharge profile for PVIMo-ZnPOM/VC/S (70% sulfur) at 0.5C using 10µl/mg of sulfur to electrolyte ratio, (c) Battery cycling performance of PVIMo-ZnPOM/C/S cathode at 0.5C over 100 cycles.

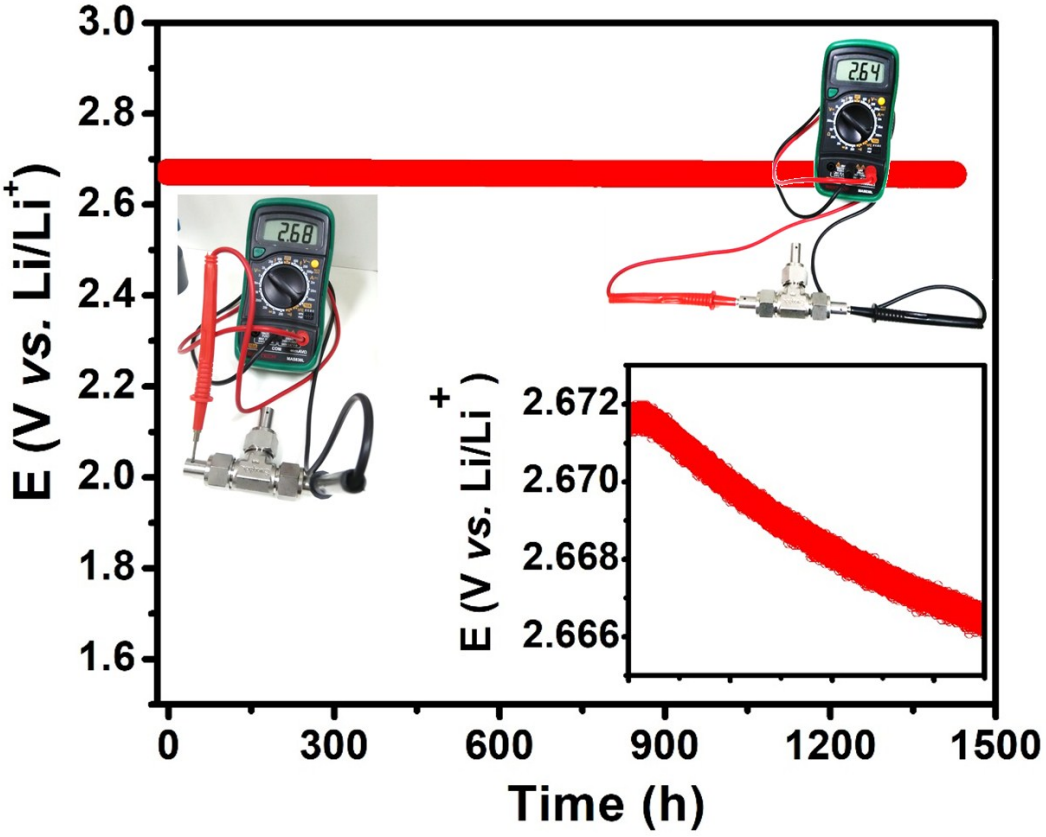

Figure S5. Monitoring of open circuit potential (OCP) of PVIMo-ZnPOM/VC/S (70%) cathode after stabilization for 3 days along with photographic images which were collected before and after continuous running the OCP monitoring for two months.

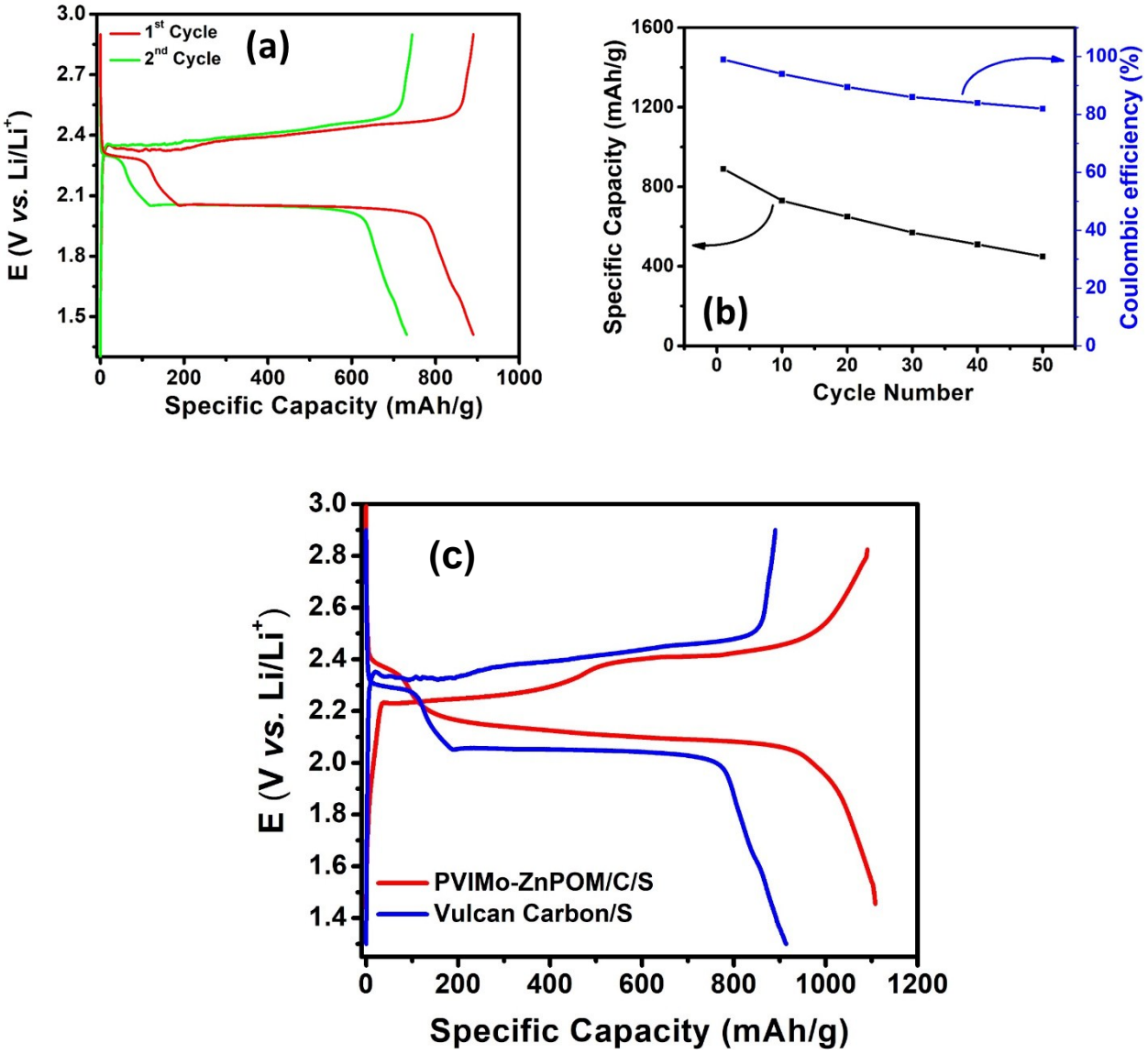

Figure S6. (a) Galvanostatic discharge-charge profile and (b) cycling performance along with coulombic efficiency for VC/S cathode at 1C. (c) Galvanostatic charge-discharge profile of PVIMo-ZnPOM/C/S and VC/S cathode at 1C.

Table S1: Comparison of Various cathode performance for Li-S battery (in term of Areal Capacity)			
S. No.	**Cathode material**	**Areal Capacity (mAh cm^{-2})/C rate**	**Ref.**
1	Flexible and multilayer nanocarbon-	6.2/0.1C	5
2	Hierarchical carbon nanotube	6.5/1C	6
3	MWCNT porous microspheres	-	7
4	MWCNT porous microspheres	4.5/0.1C	8
5	N,O-codoped porous hollow carbon fibers	6.2/ 0.3C	9
6	3D Carbonaceous Current Collectors	3/0.2C	10
	3D porous CNT sponges	13.3 / cd 16 mA/cm2	22
	nitrogen-doped graphene welded in the carbon nanotube/nanofibrillated cellulose (CNT/NFC) framework	8 / 0.5 C	23
	porous nitrogen-doped carbon fiber foam	8.7 (sulfur loading of 7.7 mg cm^{-2})	24
12	**PVIMo-ZnPOM/S/C**	**11/0.5C**	**This work**

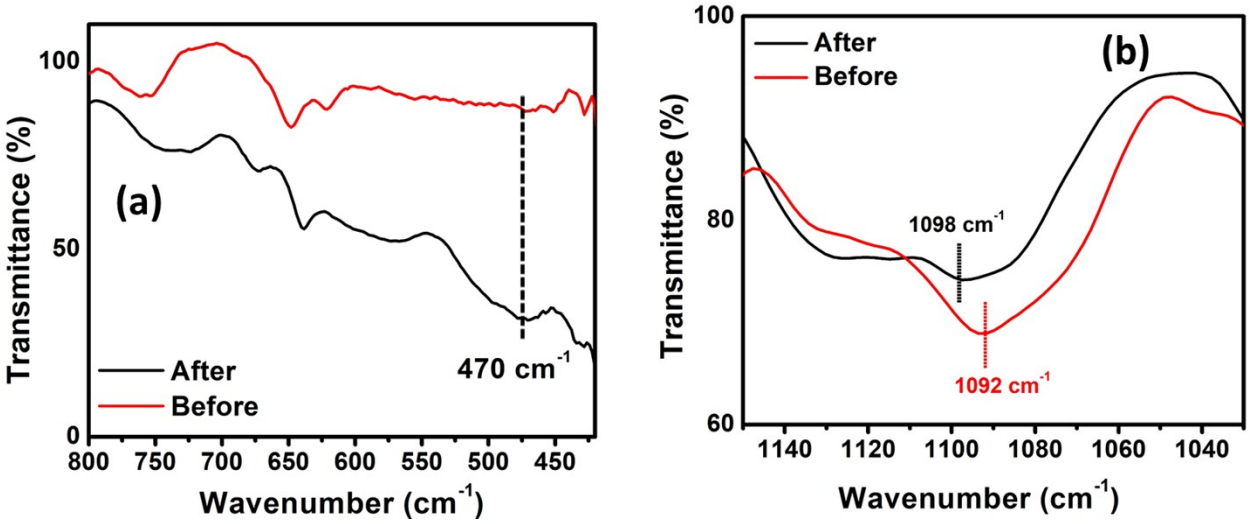

Figure S7. (a) FT-IR analysis showing the incorporation of Li_2S_4 (S-S linkage) and (b) shift in the C-O stretching frequency before and after Li_2S_4 adsorption.

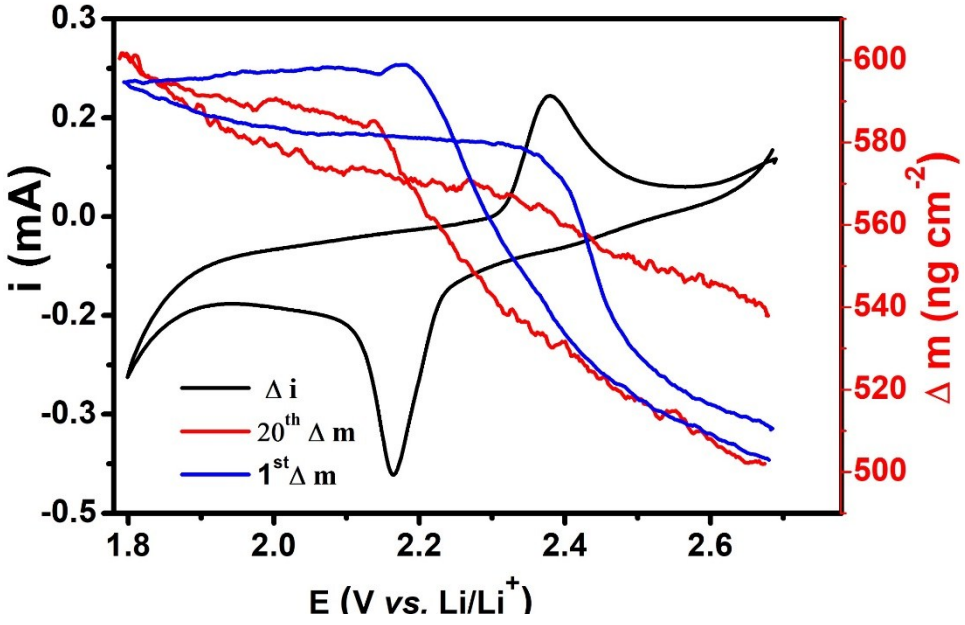

Figure S8. Cyclic voltammogram and corresponding comparative mass change of PVIMo-ZnPOM/C/S cathode during intercalation and de-intercalation process after 1st and 20th cycle.

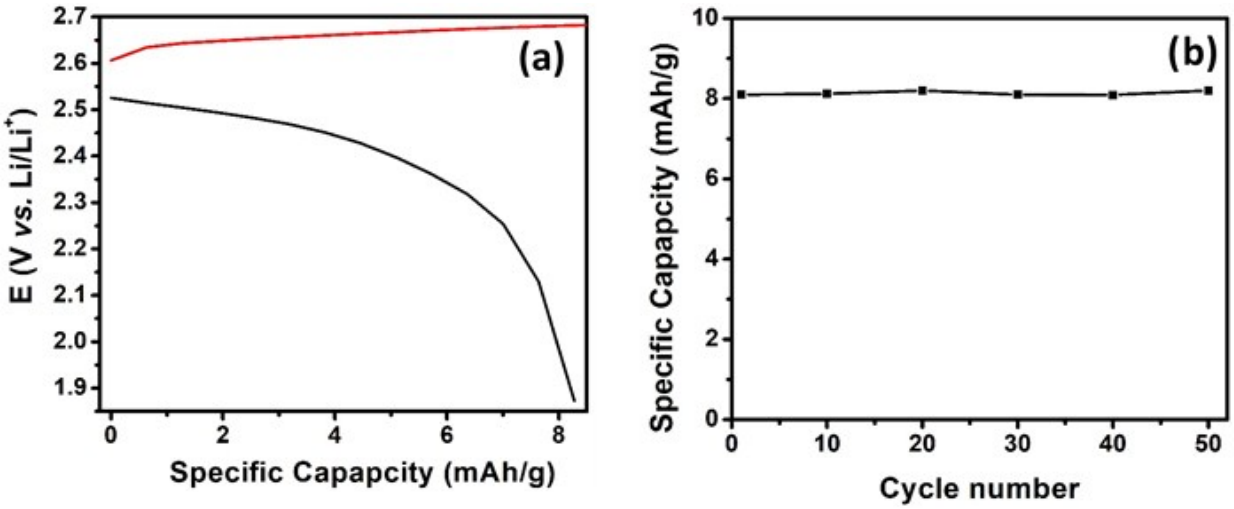

Figure S9. (a) Galvanostatic discharge-charge profile and (b) cycling performance for PVIMo-ZnPOM composite without sulfur as cathode material at 1C.

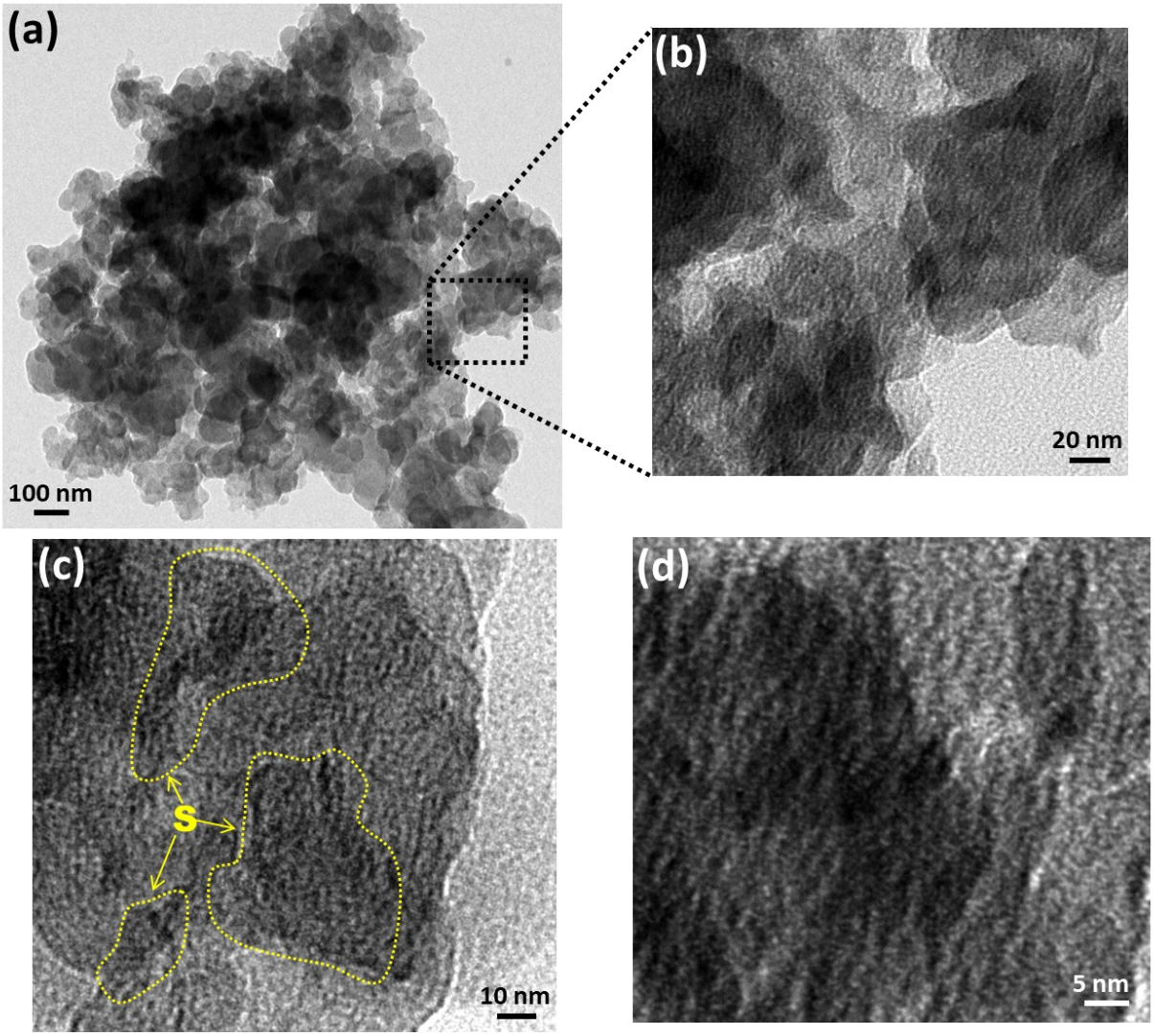

Figure S10. (a and b) TEM and (c and d) HR-TEM images at different magnification for PVIMo-ZnPOM/C/S.

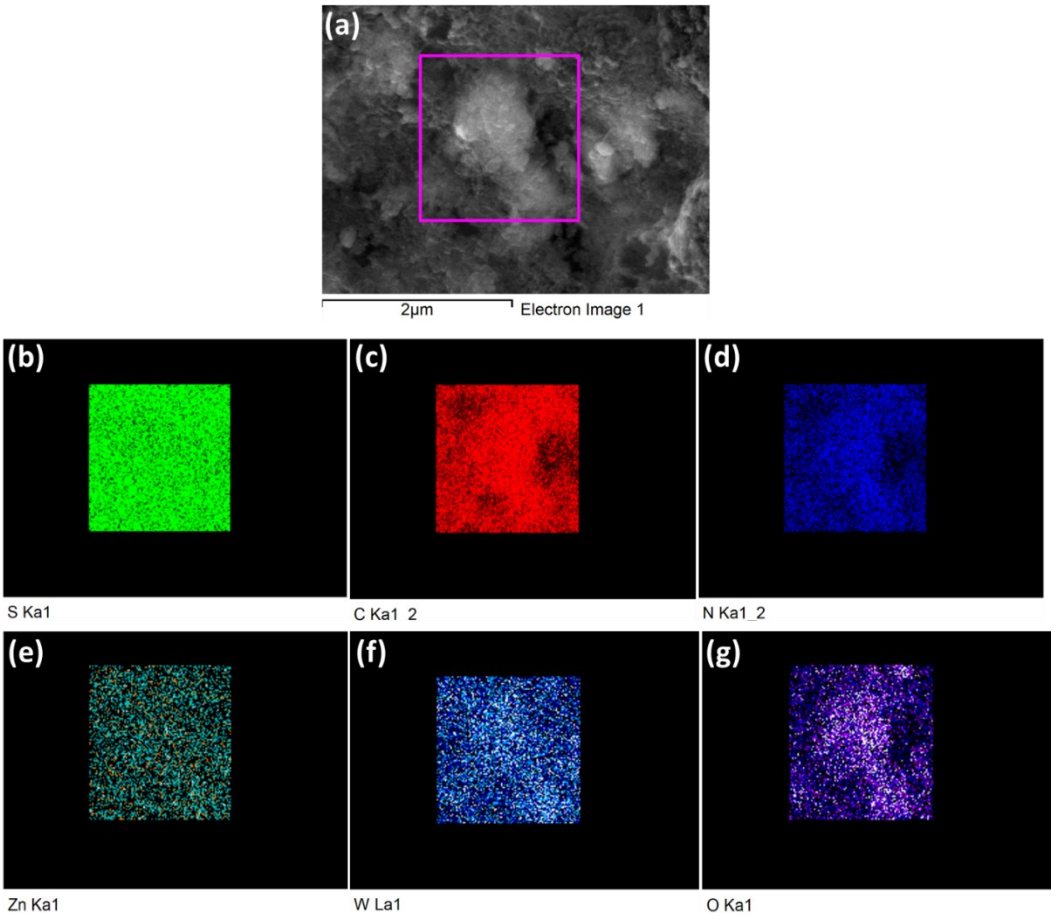

Figure S11. Elemental dot mapping analysis for (a) PVIMo-ZnPOM/C/S cathode in the discharged state showing the presence of (b) sulfur, (c) carbon, (d) nitrogen, (e) zinc, (f) tungsten and (g) oxygen.

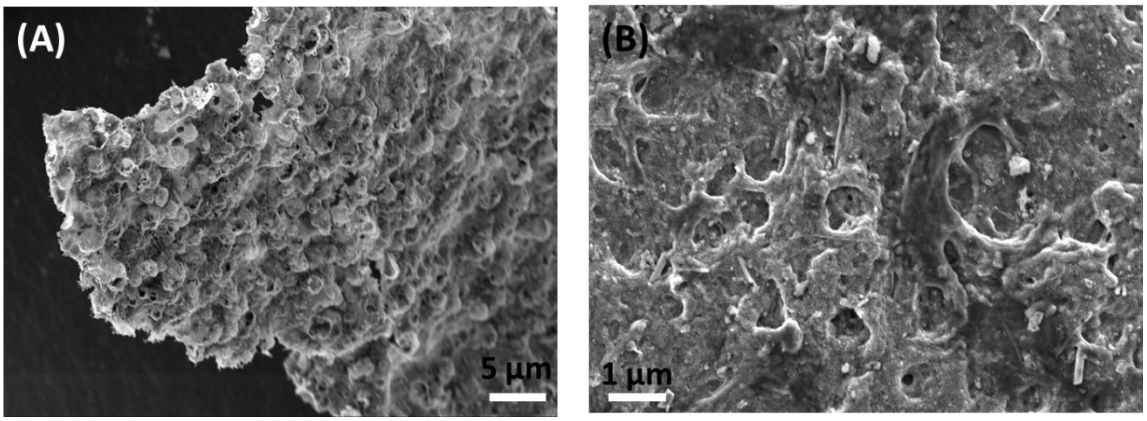

Figure S12. SEM image of VC/S cathode (a) pristine and (b) after discharge process.

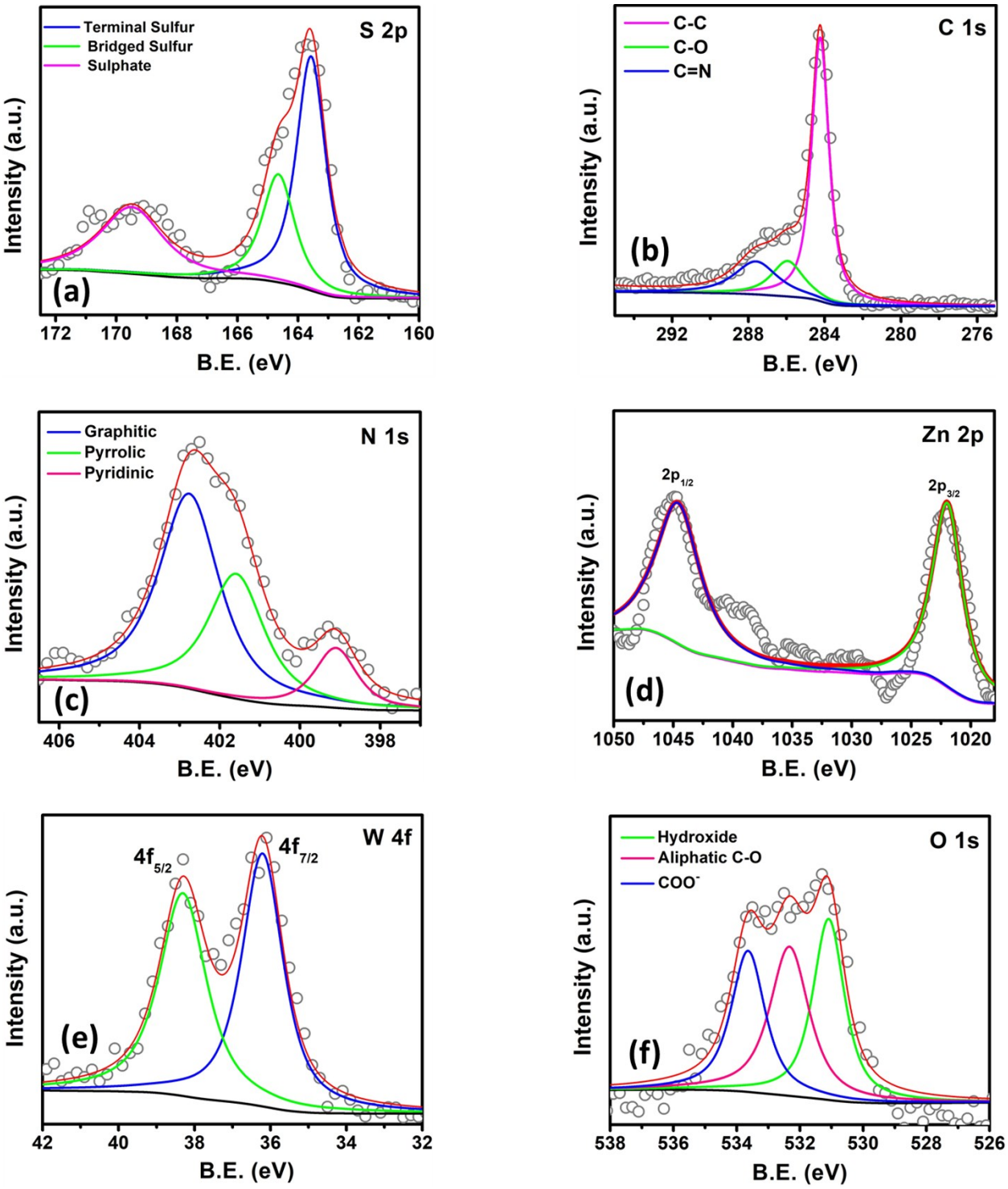

Figure S13. XP spectra for (a) S 2p, (b) C 1s, (c) N 1s, (d) Zn 2p, (e) O 1s and (f) W 4f of PVIMo-ZnPOM/C/S cathode after 120 charge-discharge cycle.

Solid State UV-Vis analysis:

Concentration of LiPS = 10^{-5} M

Volume of the prepared solution = 5 mL or 5000 µL

5000 µL of solution contain dissolved LiPS = 7 mg

1 µL of solution contain dissolved LiPS = $\frac{7\ mg}{5000\ \mu l}$ µL

80 µL of solution contain dissolved LiPS = $\frac{7\ mg}{5000\ \mu l} \times 80$ µL = 0.11 mg

Loading at the cathode 2.20 mg, and the amount of sulfur content loaded = 1.32 mg

Loss of sulfur in the form of LiPS = 0.11 mg

$$\% \text{ loss} = \frac{0.11\ mg}{1.32\ mg} \text{x } 100 = 8.3\ \%$$

From the above calculation loss in sulfur was found to be 8.3 % after 120 discharge-charge cycles which is responsible for the facile interaction and conversion of LiPS onto the surface of electrode.

Potentiometric titration:

In order to estimate the amount of dissolved sulfur in the electrolyte solution, potentiometric titration was performed after 120 charge-discharge cycles by following the previously reported procedure.[11] Briefly, the titration was performed using Ag/Ag_2S as sensor electrode and 0.01 M $AgNO_3$ as titrating agent. In order to estimate the different form of sulfur, obtained LiPS was treated with ascorbic acid under alkaline condition.

The reaction involved in the potentiometric titration is as follows;

$$Li_2S + AgNO_3 \rightarrow LiNO_3 + Ag_2S$$

The following calculation gives sulfide in grams per liter (g/L);

$$Li_2S = 45.95 \times 0.005 = 0.113 \text{ g/L}$$

Volume of $AgNO_3$ consumed during the titration = 0.75 mL

Total Volume of Li_2S solution taken = 3 mL

$$\frac{ml\ of\ AgNO3\ of\ 0.005\ N}{ml\ of\ sample} \times 0.113\ \text{g/L} = \frac{0.75\ ml}{3\ ml} \times 0.113\ \text{g/L} = 0.028\ \text{g/L}$$

$$\text{Molarity} = \frac{0.028}{45.95} = 0.0006\ \text{M}$$

$$\text{Weight} = \frac{0.0006 \times 45.95 \times 3}{1000} = 0.08\ \text{mg}$$

Loading at the cathode = 2.0 mg and the corresponding amount of sulfur = 1.2 mg

Loss of sulfur in the form of LiPS = 0.08 mg

$$\%\ \text{loss} = \frac{0.08}{1.2} = 6.6\ \%$$

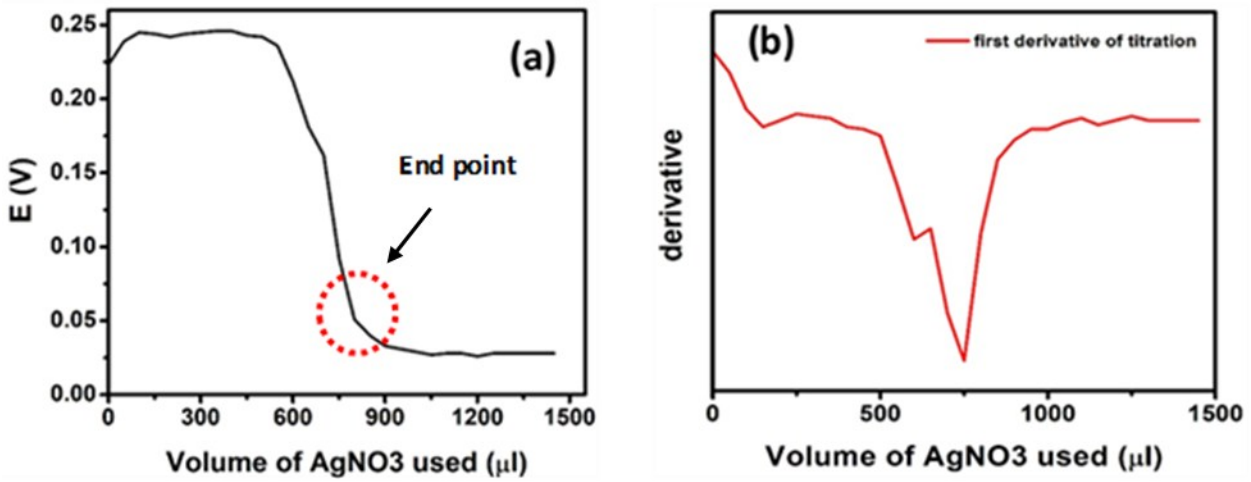

Figure S14. (a) Potentiometric titration curve and its (b) first derivative plot for LiPS in DME-DOL electrolyte (1:1 ratio v/v) after 120 galvanostatic charge-discharge cycles using Ag_2S as sensor electrode for LiPS and 0.01 M $AgNO_3$ as titrating agent.

Utilization of sulfur (Calculation)

$$\text{Sulfur utilization} = \frac{Specific\ Capacity\ in\ last\ cycle}{Specific\ Capacity\ in\ first\ cycle} * Coulombic\ efficiency\ in\ last\ cycle$$

For PVIMo-ZnPOM/C/S;

$$\text{Sulfur utilization} = \frac{1060\ mAh/g}{1090\ mAh/g} * 98.3\ \% = 95.6\ \%$$

For VC/S;

$$\text{Sulfur utilization} = \frac{450\ mAh/g}{890\ mAh/g} * 82\ \% = 41.2\ \%$$

Adhesion Property: To understand the binding ability of PVIMo in the cathode, the adhesion strength of cathode (PVIMo-ZnPOM/C/S) with Aluminium collector was studied by lap-shear test using a Tinius Olsen H50KS universal tensile testing machine. Aluminium substrates of dimension (60 mm×12 mm×0.07 mm) were used to prepare the test specimens. The surface of the substrates was cleaned using acetone. The composites materials were adhered between the two substrates with lap length of 15 mm. The specimens were extended at 0.1 mm/min at room temperature. All measurements was repeated at least 5 times for each sample. Figure S15 shows the force *vs* displacement where in the cathode exhibit plot which exhibit up to 3.6±0.2 N force with extension of 0.3±0.05 mm.

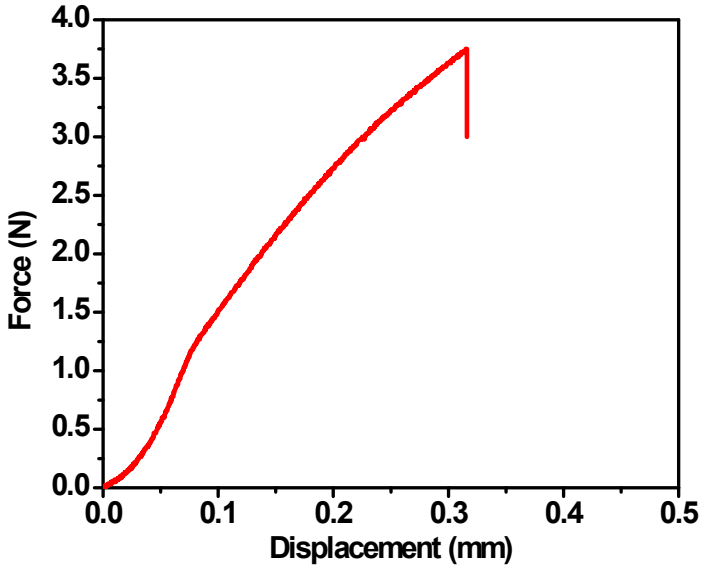

Figure S15. Force *vs* displacement plot for PVIMo-ZnPOM/C/S and current collector (Al) from lap-shear tensile testing.

Table S3: Binding energy of Li_2S_4 after adsorbed with PVIMo-ZnPOM composite derived from XPS data.

Sulfur Species	Li_2S_4 [2]	Li_2S_4/ PVIMo-ZnPOM

Table S2: Comparison of cathode performance for Li-S battery.

S. No.	Cathode material	Specific Capacity (mAh/g)/C rate	Capacity retention (No. of cycles)		Ref.
1	**PVIMo-ZnPOM/S/C**	**1080/1C**	**97% (120)**		**This work**
2	Sulfur wire/Carbon nanoparticles	675/0.1C	83% (100)		12
3	N,O dual doped porous carbon	1155/0.2C	62% (600)		13
4	CuS quantum dot/Carbon aerogel	1318/0.2C	81% (100)		14
5	ZnO/S/Carbon nanotubes	1663/0.16 A/g	57% (70)		8
6	S/$FePO_4$/Graphene oxide	1338/1C	45.5% (100)		15
7	Nd_2O_3/Carbon aerogel	1343/0.2C	81% (100)		16
8	MoS_{2-x} /r-GO/S	1200/0.5C	49% (600)		17
9	KB@Ir	980/1C	45% (100)		18
10	Ni film on Al	750/0.1C	93% (100)		19
11	Pt/C	1100/0.1C	72% (100)		20
12	Fe/porous graphene microstrucutre	700/2C	71% (500)		21
13	2D MoN-VN	708 @ 2 C		sulfur loading of 3.0 mg cm	25
14	polypyrrole @ metal–organic frameworks	670 and 440 @ 10.0 C after 200 and 1000 cycles		sulfur loading of 50 wt%	26
15	Nickel–Iron Layered Double Hydroxide	1091 mAh g^{-1} @ 0.2 C			27

Terminal Sulfur	161.4 eV	164.05 eV
Bridged Sulfur	163.4 eV	164.9 eV

References:

1. V. Singh, S. D. Adhikary, A. Tiwari, D. Mandal, T. C. Nagaiah, *Chem. Mater.*, **2017**, *29*, 4253-4264.
2. H. Yao, G. Zheng, P.-C. Hsu, D. Kong, J. J. Cha, W. Li, Z. W. Seh, M. T. McDowell, K. Yan and Z. Liang, *Nat. Chem.*, **2014**, 5,3943.
3. A. Manthiram, Y. Fu, Y.-S. Su, *Acc. Chem. Res.*, **2013**, *46*, 1125-1134.
4. A. Tiwari, T. C. Nagaiah, *ChemCatChem*, **2016**, *8*, 473-473.
5. H. Shi, S. Niu, W. Lv, G. Zhou, C. Zhang, Z. Sun, F. Li, F. Kang, Q.-H. Yang, *Carbon*, **2018**, *138*, 18-25.
6. R. Carter, B. Davis, L. Oakes, M. R. Maschmann, C. L. Pint, *Nanoscale*, **2017**, *9*, 15018-15026.
7. X. Ye, J. Ma, Y.-S. Hu, H. Wei, F. Ye, *Mater. Chem. A*, **2016**, *4*, 775-780.
8. X. Gu, C.-j. Tong, B. Wen, L.-m. Liu, C. Lai and S. Zhang, *Electrochim. Acta*, **2016**, *196*, 369-376.
9. L. Qie and A. Manthiram, *Chem. Commun.*, **2016**, *52*, 10964-10967.
10. H.-J. Peng, W.-T. Xu, L. Zhu, D.-W. Wang, J.-Q. Huang, X.-B. Cheng, Z. Yuan, F. Wei and Q. Zhang, *Adv. Funct. Mater.*, **2016**, *26*, 6351-6358.
11. V. Kolosnitsyn, E. Kuzmina and E. Karaseva, *J. Power Sources*, **2015**, *274*, 203-210.
12. P. J. Hanumantha, B. Gattu, P. M. Shanthi, S. S. Damle, Z. Basson, R. Bandi, M. K. Datta, S. Park, P. N. Kumta, *Electrochim. Acta*, **2016**, *212*, 286-293.
13. N. Jayaprakash, J. Shen, S. S. Moganty, A. Corona and L. A. Archer, *Angew. Chem*, **2011**, *123*, 6026-6030.
14. X. Li, K. Hu, R. Tang, K. Zhao and Y. Ding, *RSC Advances*, **2016**, *6*, 71319-71327.
15. Y. Lu, Y. Huang, Y. Zhang, Y. Cai, X. Wang, Y. Guo, D. Jia, X. Tang, *Ceramics International*, **2016**, *42*, 11482-11485.
16. X. Li, L. Zhang, Z. Ding, Y. He, *J. Electroanal. Chem*, **2017**, *799*, 617-624.
17. H. Lin, L. Yang, X. Jiang, G. Li, T. Zhang, Q. Yao, G. W. Zheng, J. Y. Lee, *Energy Environ. Sci.*, **2017**, *10*, 1476-1486.
18. P. Zuo, J. Hua, M. He, H. Zhang, Z. Qian, Y. Ma, C. Du, X. Cheng, Y. Gao, G. Yin, . *Mater. Chem. A*, **2017**, *5*, 10936-10945.
19. G. Babu, K. Ababtain, K. S. Ng, L. M. R. Arava, *Sci. Rep*, **2015**, *5*, 8763.
20. H. Al Salem, G. Babu, C. V. Rao, L. M. R. Arava, *J. Am. Chem. Soc.*, **2015**, *137*, 11542-11545.
21. C. Zheng, S. Niu, W. Lv, G. Zhou, J. Li, S. Fan, Y. Deng, Z. Pan, B. Li, F. Kang, *Nano Energy*, **2017**, *33*, 306-312.
22. G. Yang, J. Tan, Jian, J. Ho, Y. H. Kim, X. Yang, D. H. Son, S. Ahn, H. Zhou, C. Yu, *Adv. Funct. Mater.*, **2018**, *28*, 1800595.
23. M. Yu, J. Ma, M. Xie, H. Song, F. Tian, S. Xu, Y. Zhou, B. Li, D. Wu, H. Qiu, R. Wang, *Adv. Energy Mater.* **2017**, *7*, 1602347.
24. S. Y. Zhao, R. P. Fang, Z. H. Sun, S. G. Wang, J.-P. Veder, M. Saunders, H.-M. Cheng, C. Liu, S. P. Jiang, F. Li, *Small Methods* **2018**, *2*, 1800067.
25. C. Ye, Y. Jiao, H. Jin, A. D., Slattery, K. Davey, H. Wang, S. Qiao, *Angew. Chem. Int*. Ed. **2018**, doi:10.1002/anie.201810579
26. H. Jiang, X.-C. Liu, Y. Wu, Y. Shu, X. Gong, F.-S. Ke, H. Deng, *Angew. Chem. Int. Ed.* **2018**, *57*, 3916.
27. J. Zhang, Z. Li, Y. Chen, S. Gao, X. W. (. Lou, *Angew. Chem. Int. Ed.* **2018**, *57*, 10944.